Preparation of VOC low-temperature oxidation catalysts with copper and iron binary metal oxides via hydrotalcite-like precursors

Hongwei Zhang[a,b], Jianjun Li[a,b*], Song Shu[a,b], Jiaxiu Guo[a,b], Yongjun Liu [a,b], Wanglai Cen[a,c],

Xinpeng Li[d], Jianrong Yang[d]

[a] *National Engineering Research Center for Flue Gas Desulfurization, Sichuan University, Chengdu 610065,*

China

[b] *College of Architecture and Environment, Sichuan University, Chengdu 610065, China*

[c] *Institute of New Energy and Low Carbon Technology, Sichuan University, Chengdu 610065, China*

[d] *Chongqing Iron & Steel Company Limited，Chongqing 401220，China*

---

[*] Corresponding authors at: College of Architecture and Environment, Sichuan University, Chengdu 610065, China.

  Tel./fax: +86 13908186327, E-mail address: jjli@scu.edu.cn (Jianjun Li)

S1. Titration curve experiment

Titration curve experiments were conducted to understand the precipitation of metal salt solution under different pH values and to further explore the effects of pH conditions on hydrotalcite synthesis. In the experiment, metal solutions with different metal molar ratios were used as solution A. Liquid B was precipitated with a molar ratio of NaOH to Na2CO3 of 1 and a concentration of 2M. Liquid B was gradually titrated down at room temperature by continuously stirring the system and the pH value was recorded to plot the titration curve. The experimental results are shown in Fig. S1.
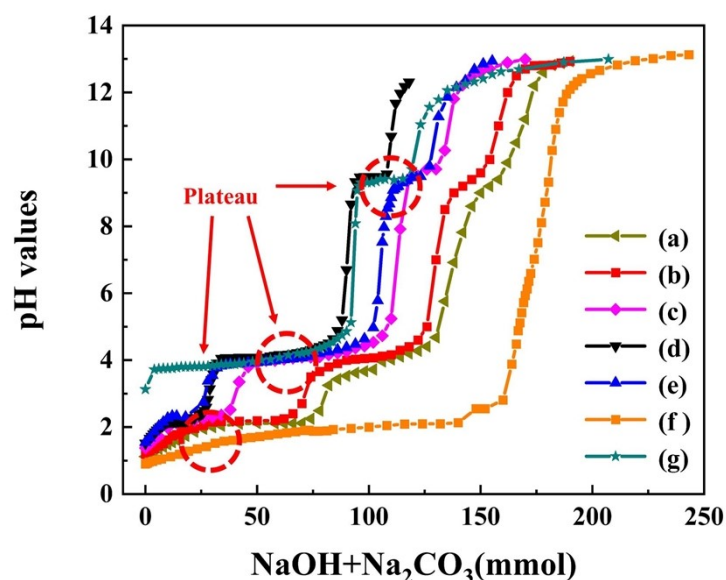

Fig. S1. Titration curves of Cu/Fe=1(a), Cu/Fe=2(b), Cu/Fe=3(c), Cu/Fe=4(d), Cu/Fe=5(e), Fe(NO$_3$)$_3$(f), Cu(NO$_3$)$_2$(g)

In the experimental results, there were three obvious titration plateau regions corresponding to pH = 1.7-2.7, 3.7-5, and 9-9.8, respectively. The titration curves showed a clear trend with the increase in copper content. The phenomenon of titration plateau is related to the solubility product of hydroxides corresponding to metal elements. Combined with the information on the solubility products of hydroxides of

some metal ions listed in Table S1, the first plateau of 1.7-2.7 is consistent with the precipitation range of Fe^{3+}. It can be concluded that this region is mainly caused by precipitation of $Fe(OH)_3$, which is consistent with the findings by Jadhav. et al [1]. At this point, Cu^{2+} precipitation does not occur and therefore co-precipitation does not occur, which is not applicable to the synthesis with hydrotalcite structures. However, the precipitation of Cu^{2+} and Fe^{3+} may occur in the pH range corresponding to the other two plateaus, which may be formed due to the depletion of alkali solution caused by the formation of hydrotalcite structure. However, it is noteworthy that the precipitation of Mg^{2+} in the conventional hydrotalcite-Mg-Al system requires a pH greater than 8.63 to achieve co-precipitation compared to the Cu-Fe system, which is why the preparation of conventional hydrotalcite materials requires an alkaline environment as the basic condition, while Cu and Fe containing hydrotalcite can be prepared under acidic conditions. Therefore, in this study, the pH values of 4.5 and 9.5 were selected to specifically explore the preparation of Cu-Fe-LDH.

Table S1

Hydride solubility product information table of metal elements

Element	Mg^{2+}	Al^{3+}	Cu^{2+}	Fe^{3+}
Solubility product (298K)	1.8×10^{-11}	3×10^{-34}	2.2×10^{-20}	4×10^{-38}
pH at the beginning of precipitation (a[Mn+]=1mol/L)	8.63	2.83	4.17	1.53
pH at complete precipitation (a[Mn+]=10^{-5}/L)	11.13	4.49	6.67	3.2

S2. The process of catalysis preparing

Fig. S2. The Schematic diagram of the process of preparing

The Cu and Fe catalysts prepared by co-precipitation method are shown in Fig. S2. Copper nitrate ($Cu(NO_3)_2 \cdot 3H_2O$) and ferric iron nitrate ($Fe(NO_3)_3 \cdot 9H_2O$) were mixed in a metal salt solution A with a mole ratio of Cu to Fe of 2. Solution B was prepared from sodium hydroxide (NaOH) and sodium carbonate (Na_2CO_3) in a molar ratio of 1:1 at a concentration of 1 M. The 100 mL distilled water was prepared as solution C. The precursor was prepared by the method of low degree of supersaturation: Solution A was slowly dripped into solution C by a peristaltic pump at 10mL/min at room temperature. Solution B was used to adjust the pH of the solution to maintain it at 4.5±0.2 or 9.5±0.2, during the drip-adding process. After the addition was completed, the mixture was kept stirred for 30 min, placed in a water bath, and reacted at 80 °C for 12 hr. After cooling at room temperature, the mixture was repeatedly washed with distilled water until it became neutral and dried overnight at 110 °C, the precursors named CuFe-P-4.5 and CuFe-P-9.5 were obtained, and monometallic oxide precursors named Cu(OH)x and Fe(OH)x were prepared by the same method at pH = 9.5 to further compare the Cu and Fe metal interactions. The precursor was calcined at

400℃for 4h, and then the solid was grounded and sieved from 0.5mm to 1mm as the catalysts.

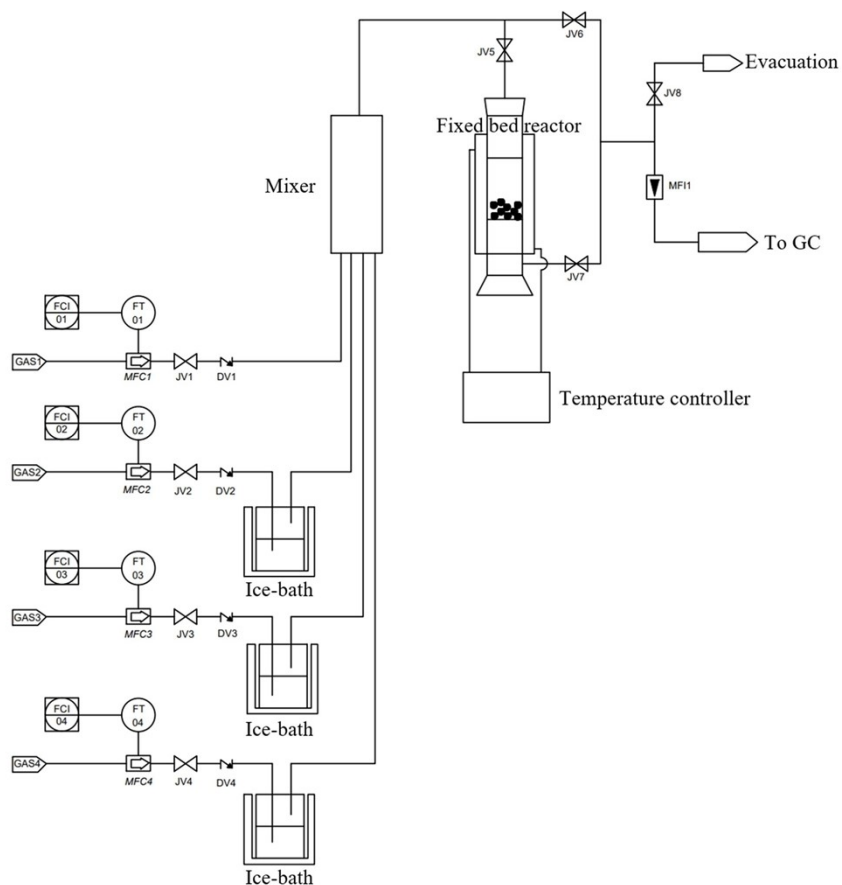## S3. The test device of catalytic performance

Fig. S3. Schematic diagram of the catalytic efficiency test system of catalyst

Catalytic performance was evaluated in a fixed-bed reactor shown in Fig. S3. The reactor was made of a quartz tube with an inner diameter of 8 mm. The VOC emissions from the spraying and drying process in the spraying industry were the foundation for the simulated gas parameters in this experiment. The inlet toluene concentration was set at 1000 ppm. The total flow rate of toluene and air was set at 550 mL/min. The gas hourly space velocity (GHSV) was controlled at 30000 h^{-1}. A thermocouple was used to control and monitor the temperature. Gas concentration

was analyzed by gas chromatography coupled with a flame ionization detector (FID, GC-2000III, Shanghai Shangjiqunli Analytic Instrument Co., Ltd.). The temperature range of this experiment was 200-330°C and the concentration was noted when the temperature was stable and the difference between before and after the measurement was less than 5%.

S4. The detail of characterization information

X-ray diffraction (XRD) analysis of sample was performed to understand the construction of crystal, which is the main analytical tools of LDH, using the Bruker D8 ADVANCE diffractometer instrument, with Cu K constant radiation (λ =0.15418nm), at a step length of 0.02°, a speed of 0.12°/ step, and a range of 2 θ from 5° to 80° (40KV, 40mA).

The chemical bonds and surface acid functional groups of the sample were studied by Fourier Transform Infrared Spectroscopy (FT-IR). FT-Infrared spectra of samples in KBr matrix were recorded on a Thermo Fisher Nicolet Is10 FTIR spectrometer in the range 4000 to 400 cm^{-1}.

The sample morphology was examined using scanning electron microscopy (SEM, JEOLJMF-7500 F, Japan), coupled to an Oxford INCA EDX detector system operation at 12kV and 15mA.The sample microstructure was examined by using Transmission Electron Microscope (TEM, JEOL-JEM2100 Plus, Japan Electronics Co., LTD,).

Thermal stability analysis was carried out by TG experiment (SDTQ600, TA USA). The data from room temperature to 800°C were measured at a heating rate of 10°C/min under high purity nitrogen.

The texture paraments were determined by N_2 adsorption desorption method at liquid nitrogen temperature using AUTOSORB-IQ (Quantachrome, USA). Prior to the measurement, all the samples were degassed at 180℃ at 10-6 Torr for 6 h. The surface area (BET) was calculated by Brunauer-Emmett-Teller(BET) equation for adsorption curves with relative pressures ranging from 0.05 to 0.35. For the calculation of total pore volume, the N_2 adsorption capacity corresponding to the relative pressure of 0.95 was selected. The pore size distribution was calculated using density functional theory (DFT) from the desorption curve.

A TP-5076 chemisorption analyzer (Tianjin First Industry and Trade Development Co., Ltd., China) was used to perform the H_2-temperature-programming reduction (H_2-TPR) experiments, and further to investigate the redox ability of catalyst. The samples (50mg) were pretreated under He for 1h to remove any impurities and water adsorbed on the surface and then cooled to 50℃. The temperature was ramped to 800℃ (5℃/min) in the presence of a gas mixture comprising 5 vol% H_2 in N_2 (30mL/min).

The temperature-programmed desorption of oxygen (O_2-TPD) was done using the same apparatus. The sample (50mg) was treated with He for1 h. After cooling to 50℃, 3 vol% O_2-He gas was passed in for 1 h. After the O_2 adsorption was saturated, a He purge for 1 h removed the physically adsorbed O_2. The samples were then heated to 800℃ under He for testing.

The surface elements and their valence states of the sample can be analyzed with X-ray photoelectron spectroscopy(XPS). Thermo Scientific EscaLab 250Xi X-ray energy spectrum was used as the excitation source with Al Ka (HV = 1486.6EV) monochromatic rays with an acceleration power of 12kW and a current of 12mA. Before test, the sample was vacuumed in the UHV tube ($<5\times10^{-7}$ Pa). The calibration criteria are Au 4F7/2 (84.0eV) and Ag 3D5/2 (368.30eV). The peak area of characteristic peak and satellite peak is calculated by the difference between gaussian curve and background curve.

S4. The economy compared of elements

Compared to most metallic elements, especially precious metals, Cu and Fe are much cheaper (Table S2), and have good economic performance and potential for industrial applications.

Table S2

Economic analysis of commonly metal elements which prepared catalyst

Element	Price (CNY / mol) [a]		
	Nitrite	Surfate	chloride
Cuprum (Cu)	95.12	27.5	31.36
Ferrum (Fe)	49.29	78.4	15.68
Manganese (Mn)	37.22	13.86	15.68
Nickel (Ni)	5,699.87	6,544.97	361.29
chromium (Cr)	28,650.74	780.43.82	130.56
Cobalt (Co)	2,677.48	132.117	133.24
Cerium (Ce)	188.45	323.44	268.26
Lanthanum (La)	298.78	9,497.48	185.69

Samarium (Sm)	337.79	4,097.64	601.94
Yttrium (Y)	337.05	4,226.91	156.53
Silver (Ag)	4,856.58	6,796.24	1,387.34
Platinum (Pt)	564,870.75	/	235,924.26
Palladium (Pd)	172,932.54	359,012.62	177,132.69

[a] the date of price based on laboratory conditions, specifications, and level of quantities purchased. Data were obtained from the website of the same chemical reagent supplier.

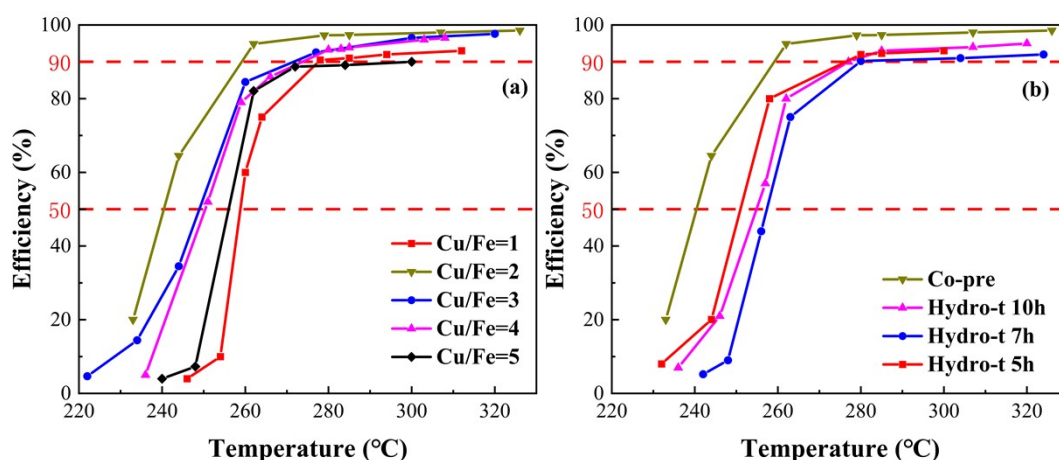## S5. Effect of preparation conditions on catalytic activity

Fig. S4. The effect from different metal molar ratios (a), and preparation methods (b) on catalytic

activity

To determine the suitable preparation conditions for hydrotalcite, the catalytic performance of toluene combustion of catalysts prepared from different metal molar ratio systems and different preparation methods was explored. The above materials were prepared at pH=4.5, and other preparation parameters were kept the same. The experimental results showed (Fig. S4(a)) that the catalyst prepared at Cu/Fe=2 condition had the best catalytic activity, and the catalytic efficiency for toluene in flue gas could reach more than 90% at 259°C. The T_{90} of the other catalysts with the order of Cu/Fe=3 (272°C) < Cu/Fe=4 (274°C) < Cu/Fe=1 (277°C) < Cu/Fe=5 (300°C). The

T_{50} with the order of Cu/Fe= 2 (240 °C) < Cu/Fe = 3 (249 °C) < Cu/Fe = 4 (250 °C) < Cu/Fe = 5 (256 °C) < Cu/Fe = 1 (259 °C). The results indicated that Cu/Fe=2 was more suitable for the preparation of catalysts, and the catalytic activity gradually decreased with the increase of the Cu/Fe molar ratio.

Fig. S4 (b) shows the activity test results of catalysts prepared by low supersaturation co-precipitation and hydrothermal methods at pH=4.5 and Cu/Fe=2 for 5h, 7h and 10h hydrothermal reactions. The catalyst prepared by the co-precipitation method achieved the removal efficiency of more than 90% toluene from flue gas at 259°C, while the same efficiency required for hydro-t 5h, hydro-t 7h, and hydro-t 10h were 276°C, 277°C and 280°C, respectively. The T_{50} of all catalysts also showed the same trend. Based on the above experimental conclusions, the material preparation parameters selected for this study were Cu/Fe=2 and the low supersaturation coprecipitation method.

S6. Catalytic performance compared with current studies

In recent years, based on the better economic performance of non-noble metals, many researchers have explored their use of them to construct catalytic combustion catalysts for VOC toluene in flue gas, as shown in Table S3. In comparison, CuFe-4.5 prepared in this study could provide higher catalytic activity for toluene in flue gas at lower temperatures.

Table S3

The catalyst activity of catalytic on toluene compared with recent studies

Entry	Catalytic	Prepared method	Reaction conditions	Efficiency	Stability	Reference
1	CeO_2-NB	Electrospinning from the precursor solution	20%O_2/N_2 and toluene with 100ppm, WHSV=60000mL $g^{-1}h^{-1}$, flow rate at 50mL/min.	T_{90}=230℃	About 90% conversion for 50 h	[2]
2	3D-Co_3O_4	The hydro-thermal method at 180℃ for 3h and calcined at 300℃ for 3h	The reactant gases (1000 ppm toluene, 20% O_2, N_2), and WHSV was usually set at 48,000mL g^{-1} h^{-1}.	T_{50}=229℃, T_{90}=238℃	Non significantly decreases for 120 h at 240℃	[3]
3	0.71wt%Na-CoCe/ZSM-5	ultrasonic-assisted impregnation and doped with Na, calcined at 450℃ for 3h.	Gas composed of 1500$\times$$10^{-6}$ toluene and air, with WHSV=20000mL/(g h)	T_{90}=250℃	/	[4]
4	OM-CoMn0.5	hydrotalcites prepared by coprecipitation as precursors to obtain the mixed oxides(OM)	Fixed bed reactor at 200mL/min, 0.2g of catalyst, and concentration of toluene of 1200ppm	T_{50} and T_{90} temperature at 217℃ and 258℃ respectively	/	[5]
5	CuO-δ-MnO_2	Facile SPF process and calcined at 400℃ for 2h	Reaction conditions: 1000 ppm toluene in air, the flow rate of 50 mL min–1, and GHSV = 30 000 mL g cat–1	T_{50}=238℃, T_{90}=258℃	above 92% for 36 h at 300℃	[6]
6	10Cu60Mn-γ Al_2O_3	Impregnation of high surface γ-Al_2O_3	1000ppm toluene in the air with a total flow rate was 200 cm^3min^{-1}(W/F=0.018g s cm^{-3})	100% conversion at ca.280℃	/	[7]
7	$Cu_6Ce_4O_x$	hydrothermal and thermal calcination	1000 ppm toluene + O_2 + N_2	T_{90}=260℃	About 90%	[8]

		method	(balance) with 60 mL/min, and SV(space velocity) is 36000mL/(g h)		conversion for 50 h at 260℃	
8	Mn$_6$/AC	the ultrasound-assisted equivalent volume impregnation method	500 ppm toluene, 6 vol% O$_2$, and pure N$_2$, with 200mL/min and GHSV is 15000 h^{-1}.	removal efficiency is 99.38% at 270 °C	remained above 81% for 30h	[9]
9	0.1MnCF-LDO/IM	KMnO$_4$ pretreating from CoFe-LDO by calcined at 400℃ for 5hr	Reaction at a Fixed-bed reactor with the flow of 100mL/min and 900ppmV toluene in20vol.%O$_2$/Ar was introduced through a 0.1g sample	T$_{50}$ and T$_{90}$ temperature at 290℃ and 316℃ respectively	within the 200min, restore gradually to 100% after the water off	[10]
10	Cu005FeKIL(30)	Two-step solvothermal synthesis and introduce Cu by impregnation	WHSV (weight hourly space velocity) of 1.2 h^{-1}, gas through a saturator filled with toluene and equilibrated at 0 °C (P$_{toluene}$ = 0.9 kPa, 1 %)	Conversion is 40% at 330℃	About 70% conversion for 200 min at 380℃	[11]

S7. The speculate of process from hydrotalcite to their derived oxides

Combined with previous research conclusions[12-15], the transformation process of hydrotalcite to prepare its derivative oxides by calcining can be divided into two or three stages, corresponding to, in general, the removal of water in the layer structure at low temperature and the removal of hydroxyl group and anion at high temperature.
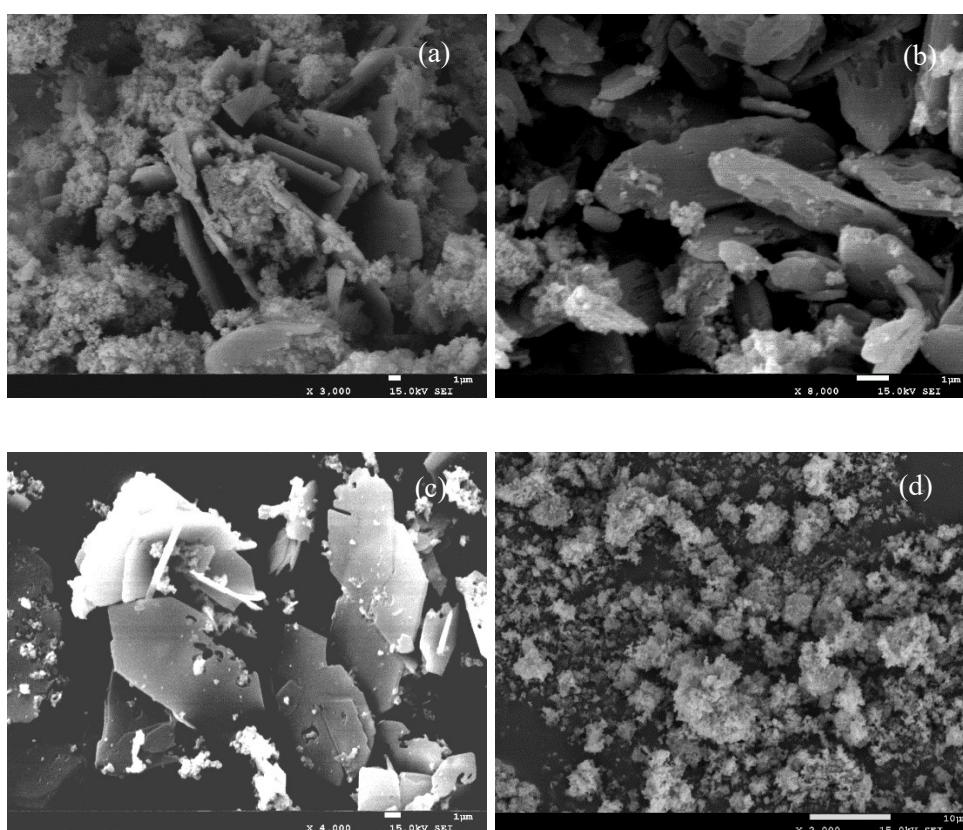

Fig. S5. SEM of CuFe-4.5 prepared from calcined at 200℃(a), 300℃(b), 400℃(c), and 500℃(d)

As research on the influence of different calcined temperatures range from 200℃ to 500℃ on the catalyst. The main structure of CuFe-4.5 did not change significantly which prepared by calcined at 200℃ shown with SEM at Fig. S5(a), and the thickness of sheet structure tended to become thinner, deformed and folded. This phenomenon

can be explained as the water adsorbed on the surface and hydroxyl groups formed at the main structure of laminates are removed gradually under the temperature, causing the flake structure to deform and shrink to a certain extent. However, the main structure characteristics of hydrotalcite can still be observed because the hydroxyl groups in most laminates are not removed, and further lead to the complete collapse of the laminates. When the temperature rises to 300℃, the SEM taken with a higher enlargement factor shown at Fig. S5(b). The structure become to forming the obvious pits at the surface of the structure, but there is still no obvious holes or cavity. To a certain extent, the collapse of the main structure of the laminate corresponds to the departure of the hydroxyl group and the interlayer anion in the layered structure. The clearer perforation phenomenon can be observed at the CuFe-4.5 prepared by 400℃ in SEM taken from different angle of view shown in Fig. S5(c). However, the serious sintering occurred when the temperature continues to rise to 500℃ shown at Fig. S5(d).

Similarly, we also compared the texture properties of CuFe-P-4.5 and the calcination preparation of its derivative oxide CuFe-4.5. The N_2 adsorption and desorption experiments and the main parameters are shown in Fig. S6 and Table S4. It can be obviously observed the surface area decreases and the average pore size increases on the basis that the total pore volume does not change significantly after calcined at high temperature.
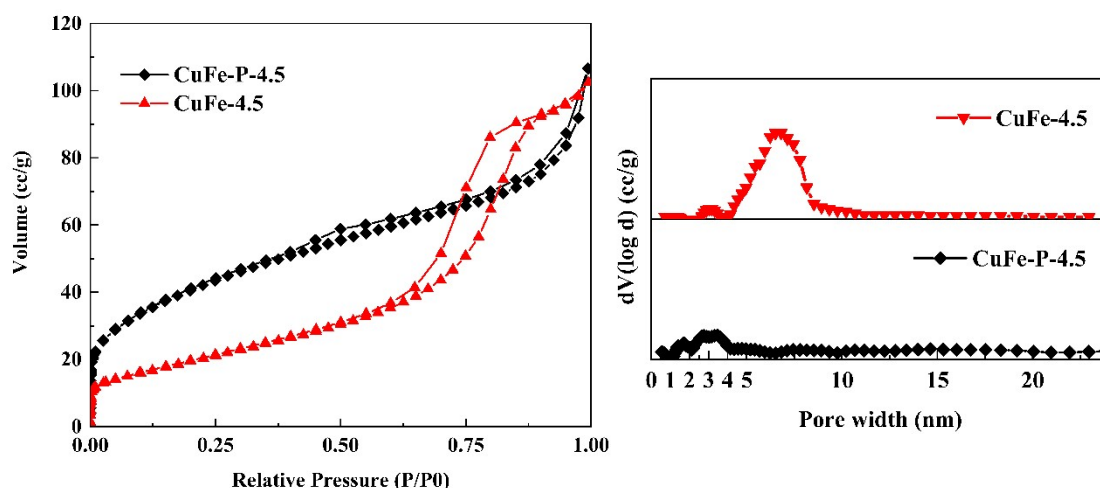
Fig. S6. N$_2$ adsorption and desorption isotherms and pore size distribution of CuFe-P-4.5 and

CuFe-4.5

Table. S4. The texture performance parameters of CuFe-P-4.5 and CuFe-4.5

Sample	Surface area (BET)/(m^2/g)	Total pore Volume/(cc/g)	Average pore Size/(nm)
CuFe-P-4.5	148.56	1.648e-1	4.44
CuFe-4.5	83.86	1.687e-1	8.05

Therefore, the conversion process of LDH with a multilayer plate-like structure to its derived oxide was speculated as following characteristics. Firstly, the hydroxyl group in the main lamellar structure of CuFe-LDH escapes from the lamellar structure rapidly under the action of high temperature, thus forming lamellar holes. The anions and water molecules between the layers quickly escape from the structural system through the channel formed by the skeleton body of Cu-O-Fe. At the same time, this process will allow the hole to continue to expand, and further increase the effective gain. The derived oxides, finally, with a stable and uniform catalyst system prepared from LDH are formed.

Reference

[1] VH. Jadhav, DK. Dumbre, VB. Phapale, HB. Borate, RD. Wakharkar. *Catal Commun*, 2007, **8**, 65-68.

[2] DF. Yan, SP. Mo, YH. Sun, QM. Ren, ZT. Feng, PR. Chen, et al., *Chemosphere,* 2020, **247**, 125860.

[3] QM. Ren, ZT. Feng, SP. Mo, CL. Huang, SJ. Li, WX. Zhang, et al., *Catal Today,* 2019, **332**, 160-167.

[4] QP. Zou, MQ. Liu, MJ. Fan, YP. Ding, YW. Chen, SB. Shen, et al., *J Rare Earth,* 2020, **39**, 409-418.

[5] DA. Aguilera, A. Perez, R. Molina, S. Moreno, et al., *Appl Catal B-Environ,* 2011, **104**, 144-150.

[6] LM. Li, JJ. Luo, YF. Liu, FL. Jing, DS. Su, W. Chu, *ACS Appl Mater Inter,* 2017, **9**, 21798-21808.

[7] SM. Saqer, DI. Kondarides, XE. Verykios, *Appl Catal B-Environ,* 2011, **103**, 275-286.

[8] L. Li, CY. Zhang, F. Chen, YT. Xiang, JL. Yan, W. Chu, *Catal Today*, 2021, **376**, 239-246.

[9] YD. Zhang, CT. Li, YC. Zhu, XY. Du, XY. Lyu, SH. Li, et al., *Fuel*, 2020, **276**, 118099.

[10] TS. Xue, RN. Li, Z. Zhang, YS. Gao, Q. Wang, *J Environ Sci*, 2020, **96**, 194-203.

[11] P. Djinović, A. Ristić, T. Žumbar, VDBC. Dasireddy, M. Rangus, G. Dražić, et al., *Appl Catal B-Environ,* 2020, **268**, 118749.

[12] WT. Reichle, *J Catal*, 1985, **94**, 547-557.

[13] P. Bera, M. Rajamathi, MS. Hegde, PV. KAMATH, *Bull Mater Sci*, 2000, **23**, 141–145.

[14] SP. Newman, W. Jones, *New J Chem*, 1998, **22**, 105-115.

[15] A. Vaccari, *Catal Today*, 1998, **41**, 53-71.